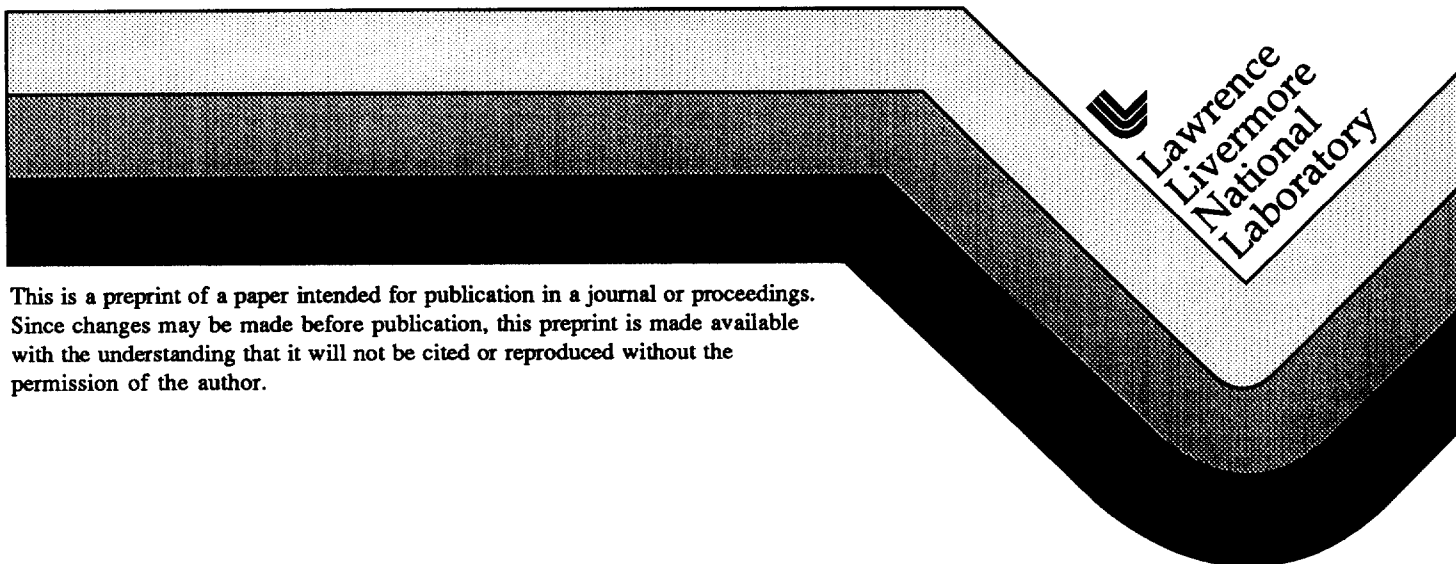


Characterization of X-ray Streak Cameras for Use on Nova

D. H. Kalantar, P. M. Bell, R. L. Costa, B. A. Hammel,
O. L. Landen, T. J. Orzechowski,
J. D. Hares, A. K. L. Dymoke-Bradshaw

This paper was prepared for submittal to the
22nd International Congress on High Speed Photography and Photonics
Santa Fe, NM
October 27-November 1, 1996

October 21, 1996



DISCLAIMER

This document was prepared as an account of work sponsored by an agency of the United States Government. Neither the United States Government nor the University of California nor any of their employees, makes any warranty, express or implied, or assumes any legal liability or responsibility for the accuracy, completeness, or usefulness of any information, apparatus, product, or process disclosed, or represents that its use would not infringe privately owned rights. Reference herein to any specific commercial product, process, or service by trade name, trademark, manufacturer, or otherwise, does not necessarily constitute or imply its endorsement, recommendation, or favoring by the United States Government or the University of California. The views and opinions of authors expressed herein do not necessarily state or reflect those of the United States Government or the University of California, and shall not be used for advertising or product endorsement purposes.

Best Available Quality

for original report

**call
Reports Library**

x37097

Characterization of x-ray streak cameras for use on Nova

Daniel H. Kalantar, Perry M. Bell, Robert L. Costa, Bruce A. Hammel,
Otto L. Landen, and Thaddeus J. Orzechowski

Lawrence Livermore National Laboratory
P.O. Box 808, Livermore CA 94550

Jonathan D. Hares and Anthony K. L. Dymoke-Bradshaw

Kentech Instruments, Ltd.
South Moreton, Didcot, Oxfordshire, OX11 9AG, UK

ABSTRACT

There are many different types of measurements that require a continuous time history of x-ray emission that can be provided with an x-ray streak camera. In order to properly analyze the images that are recorded with the x-ray streak cameras operated on Nova, it is important to account for the streak characterization of each camera. We have performed a number of calibrations of the streak cameras both on the bench as well as with Nova disk target shots where we use a time modulated laser intensity profile (self-beating of the laser) on the target to generate an x-ray comb. We have measured the streak camera sweep direction and spatial offset, curvature of the electron optics, sweep rate, and magnification and resolution of the electron optics.

Key words: x-rays, x-ray streak camera, inertial confinement fusion

1. INTRODUCTION

X-ray streak cameras record x-rays by converting them to electrons, and focusing and sweeping the electrons across an electron sensitive detector as a function of time. X-rays that are incident on the photocathode generate photo-electrons. These electrons are accelerated to 13 keV, and they are focused using electron optics onto a phosphor screen or microchannel plate detector. This 1-dimensional image that is then imaged by the electron optics is swept across the phosphor screen in time by a voltage pulse applied to sweep deflection plates at the anode aperture of the focusing optics. For the case of a phosphor screen, the phosphor fluoresces, resulting in an optical image that is then intensified and recorded on film. For the case of a microchannel plate, the electrons are detected by the microchannel plate, and an image is created by the cascade of electrons inside the microchannel plate pores, exciting a phosphor screen behind the microchannel plate.

There are several aspects of the performance of an x-ray streak camera that must be characterized in order to analyze streaked data in a quantitative way. Some characterization may be done on the bench using a low intensity DC x-ray source, such as the photocathode flat-field and the resolution of the electron-optics.

When an x-ray streak camera is run on a high power laser target shot to record data such as a time-resolved spectrum of x-ray emission from the plasma, however, it is important to understand and characterize the performance of the streak camera in a dynamic mode rather than just in a static mode. There may be electric and magnetic fields that affect the streak camera in a particular configuration when the laser beams arrive at the target, or due to the presence of other diagnostics with permanent magnets.

2. STREAK CAMERA CHARACTERIZATION

X-ray streak cameras are used on Nova target shots fielded in six-inch manipulator (SIM) re-entrant diagnostic tubes [1]. We have made modifications to the commercially available Kentech [2] design to facilitate their use in these SIM tubes. These cameras (SSCs) may be run in many different configurations. Not only may each camera may be run in different SIM locations, but the deflection plate sweep voltage pulse may be generated either with an on-board pulse generator or an external pulse generator that is located in a rack-

mounted unit external to the Nova target chamber. In addition, each pulse generator may be run with a different rise-time to generate a range of sweep rates for the streak cameras.

We use disk target shots in order to characterize the performance of the streak cameras in different SIM configurations. For these tests, we configure each streak camera with a gold photocathode, a 0.25 mm time resolution slit, and 1 mm beryllium and 50 μm titanium filtering. We place a slit array consisting of 50 μm wide slits 1.5 mm apart in front of the photocathode (Fig. 1), and then insert the streak camera into the Nova target chamber to record x-ray emission from a gold disk target. In this configuration, the slit array is 2 mm in front of the photocathode, which sits 48 cm from the disk target.

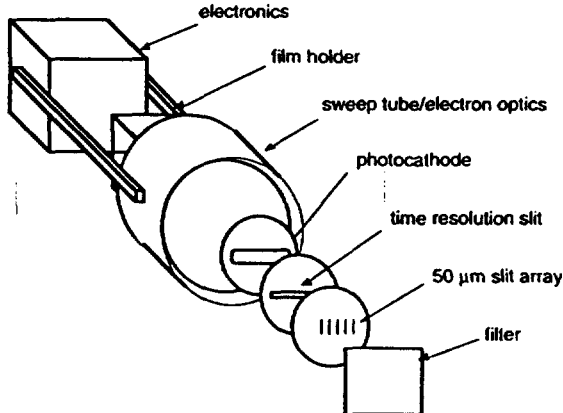


Figure 1: Setup of the SSCs for characterization on Nova disk target shots.

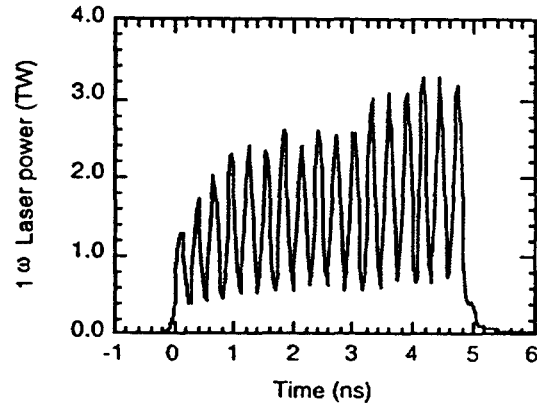


Figure 2: Laser pulse shape used to generate an x-ray comb with a gold disk target shot on Nova.

The gold disk is irradiated with a 5 ns laser pulse that has a temporal modulation generated with a 30 mm etalon inserted into the laser oscillator cavity to make the laser pulse beat. The average intensity on the disk target is $1\text{-}2 \times 10^{14} \text{ W/cm}^2$, with a self beating period of 286 ps, as shown with the 1ω laser pulse in Fig. 2.

We record the x-ray emission incident on the photocathode of the streak camera through the slit apertures in front of the photocathode. One example of the streak camera data is shown in Figure 3. Here, SSC-4 was run in SIM-7 on Nova. Time on this image sweeps vertically, shown in the figure.

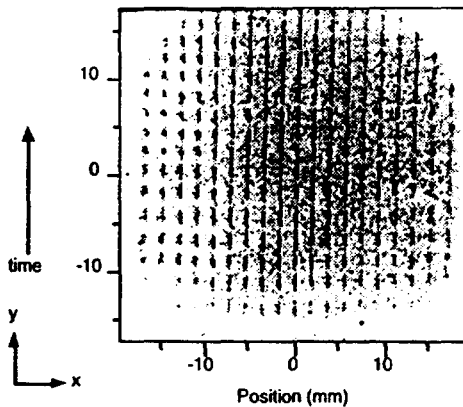


Figure 3: Film image of the streak recorded to calibrate SSC-4 in SIM-7 using a disk target shot.

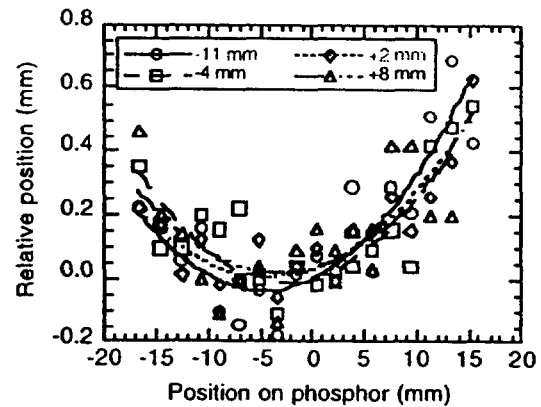


Figure 4: Polynomial fits showing the curvature of the streak data due to the electron optics.

Detailed analysis of the streak image provides calibration information for the streak camera sweep rate, sweep direction and spatial offset, resolution of the electron optics as a function of position along the photocathode, and electron optics curvature. We discuss the characterization in detail below using this streak record as an example.

2.1 Sweep direction

The sweep direction is important for analyzing data such as spectral data. For experiments that are designed to look at the shapes and positions of specific lines as a function of time, it is important to resolve apparent line shifts due to the sweep direction vs. real line shifts due to atomic physics.

The sweep direction is obtained from the emission recorded through a single slit as a function of time. The sweep direction should be square on the phosphor screen, but may not be, due to effects such as magnetic fields in the target chamber. We define the center of the phosphor screen as $x=y=0$. We then measure the x and y coordinates corresponding to the peak in x-ray emission at each beat and for each slit aperture. For the example of SSC-4 in SIM-7, the sweep direction is tilted 1.3° relative to the phosphor screen and film.

2.2 Curvature of the electron optics

The full time-space information obtained by measuring the x, y positions of the peaks of x-ray emission recorded on the phosphor screen during each beat of the laser provides a picture of the curvature of the swept image. Figure 4 shows the measured positions of the peak x-ray emission in the time direction corresponding to 4 different bursts of x-rays in the x-ray comb, as shown in the streak image in Fig. 3.

The signal that is recorded from a single burst of x-rays appears as a curved band on the film [3]. The curvature of the data is a result of the three components that add to give the overall curvature. First, the path length for x-rays to reach the photocathode varies with position along the photocathode. Second, electrons from different positions along the photocathode pass through the anode aperture and sweep plates at a range of different angles. And, third, the time delay for electrons to reach the anode aperture due to the focusing geometry of the electron optics varies with position along the photocathode.

These different effects are all approximately quadratic with distance from the center of the photocathode, but they have different magnitudes. The effect of x-ray path length difference accounts for <1 ps overall time delay in x-ray transit time to the photocathode for the SSCs used on Nova. The effect of the electron path length between the deflection plates is <2 ps. However, the delay of the arrival of electrons from the ends of the photocathode due to the field lines within the focusing optics may take up to 70 ps longer to reach the anode aperture than those generated at the center of the photocathode.

The curvature of the image may be fit by a parabola of the form

$$y = a(x - b)^2 + c$$

For the case of SSC-4 in SIM-7 we fit the parameters a, b , and c for each of the modulations in the x-ray comb. These parameters provide a definition of the curvature, which is a constant independent of sweep rate if it is expressed in terms of time. In the example of SSC-4 in SIM-7, above, the curvature a is 0.19 ps/mm^2 .

2.3 Sweep rate and offset

The parabolic fit parameters define the sweep rate as dt/dc . The etalon that is inserted into the laser oscillator cavity generates a self-beating in the laser with a fixed period of 286 ps. By plotting c as a function of time, we may do a linear fit for the average sweep rate (Fig. 5). In this case, the sweep rate is 131 ps/mm . The rate measured as $\Delta c/\Delta t$ for each pulse varies as a function of position on the phosphor. This is also shown in Fig. 5. Note that the average rate is consistent with the linear fit.

Any spatial offset, b , in the image due to the response of the electron trajectories in the sweep tube from external field effects may affect the quality of data if not properly accounted for. An example is when SSC-2 is used in SIM-6 on Nova. External magnetic fields due to the permanent magnet on the Dante diagnostic [5] cause the image to be shifted as much as 8 mm on the phosphor screen (Fig. 6). Without accurate knowledge of this offset, data near one end of the photocathode slit may be lost. There is not a significant offset for the example of SSC-4 in SIM-7.

2.4 Magnification and resolution of the electron optics

Spatial lineouts of the streak record at a fixed time provide information on the electron optics magnification and resolution. We performed lineouts at a time corresponding to the center of the phosphor

screen, $y=0$. The separation of the slits is 1.50 mm at the photocathode. The separation of the slit images on the phosphor screen indicates that there is an overall magnification in the electron optics from 1.2-1.4. This magnification as a function of position is shown in Fig. 7.

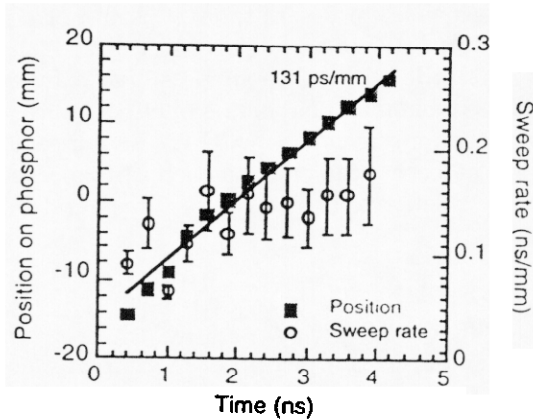


Figure 5: Linear fit of position vs. time for the x-ray comb pulses. Sweep rate is overlaid.

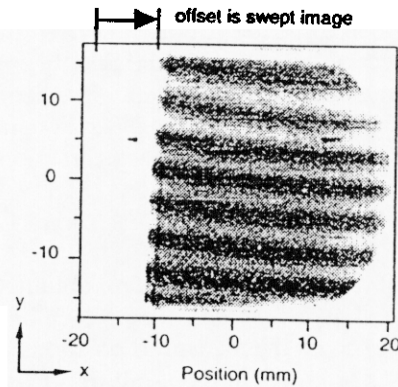


Figure 6: Streak image from SSC-2 in SIM-6 showing the offset due to magnetic fields.

By fitting the lineouts of x-ray emission recorded through each slit with a gaussian profile convolved with the 50 μm width of the slits, we obtain resolution as a function of position along the photocathode slit. This is shown in Fig. 8. In this example, the streak camera resolution is better than 150 μm over a length of about 15 mm at the phosphor, corresponding to about 12 mm at the photocathode. Note that the resolution of another camera, SSC-1, is shown in this figure with both an optical image intensifier and a microchannel plate, as discussed below.

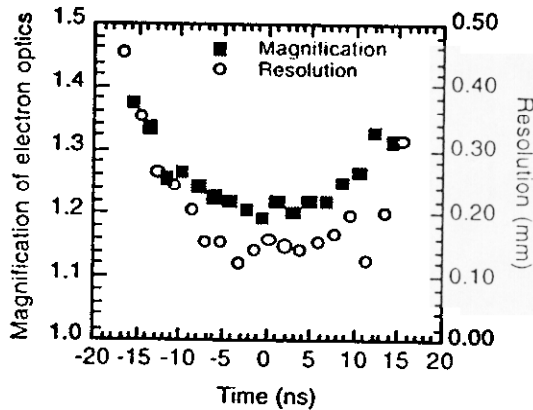


Figure 7: Magnification and resolution as a function of position on the phosphor screen.

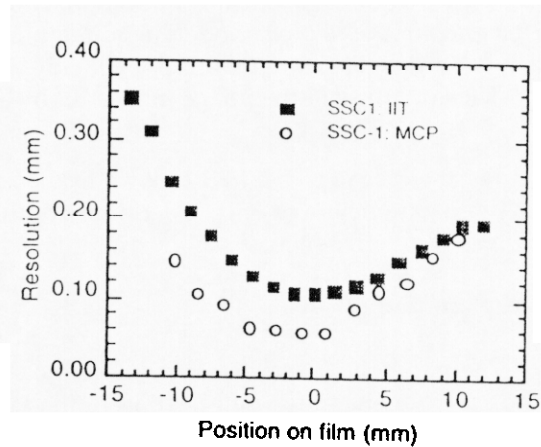


Figure 8: DC resolution of SSC-1 configured with an image intensifier vs. microchannel plate.

3. MICROCHANNEL PLATE BASED STREAK CAMERA

X-ray streak cameras that are used on Nova target experiments sometimes show a high level x-ray background. Tests that were done where the phosphor in the streak tube was rubbed off indicated that much of this background was due to the interaction of hard x-rays with the phosphor. The fluorescence in the phosphor was then amplified with the data by the image intensifier.

We replaced the optical image intensifier in one SSC with a gold coated microchannel plate in order to reduce the effect of hard x-rays interactions with the phosphor overwhelming the signal. This modification resulted in an improvement in the spatial resolution of that streak camera. Figure 8 shows the resolution of SSC-1 measured with the 50 μm slit apertures in a DC x-ray test both with an optical image intensifier and

with a microchannel plate module. The resolution is improved by about $50\text{ }\mu\text{m}$ over the full length of the photocathode.

4. EXAMPLE OF DATA ANALYSIS

The SSCs provide time resolved information with one dimension of spatial resolution. The sweep record may be used for precise measurements provided the full effects of sweep curvature and flat field are included in the analysis. We provide an example of Nova data below that relies on the details of the SSC sweep for complete analysis.

4.1 Planar foil hydrodynamics

The x-ray drive generated with a hohlraum target on Nova is used in some experiments to accelerate a planar foil in order to study the growth of instabilities such as the Rayleigh-Taylor instability. The foil package is attached to a hole in the side of the hohlraum. X-ray ablation of the modulated surface launches shocks into the package, and as it is accelerated, the modulation grows. Detailed measurements of RT growth rates are made by face-on radiography, where the modulation is measured as a modulation in optical depth in the foil in x-rays, and compared with simulation.

In order to verify that the simulations are accurate, we measure and compare the overall motion of the foil due to the x-ray drive. We measure the foil motion with an x-ray streak camera configured to image the foil in a side-on geometry, as shown in Figure 9

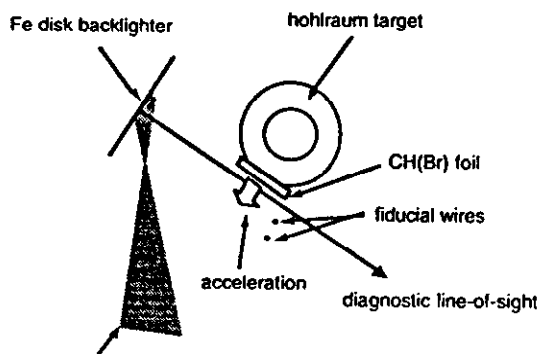


Figure 9: Schematic of the geometry for a side-on foil trajectory measurement.

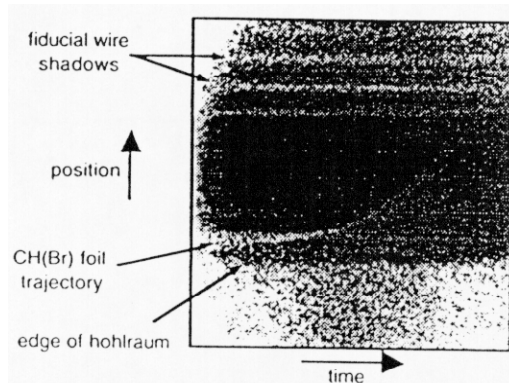


Figure 10: Streaked side-on image of a CH(Br) foil accelerated with a hohlraum x-ray drive.

One or two beams of Nova are used to generate an x-ray shadow of the foil as it is accelerated away from the side of the hohlraum. An example of a side-on foil trajectory recorded at about 30X magnification is shown in Figure 10. In this case, we accelerated a $40\text{ }\mu\text{m}$ thick CH(Br) foil with the x-ray drive from a shaped 2.2 ns laser pulse in a standard Nova hohlraum.

Fiducial wires were mounted on the target near the foil. These wires cast a shadow in the image, providing an accurate calibration for the magnification of the streak image and the sweep direction on the shot. The duration of the laser pulse used for the imaging is recorded in x-ray emission. This provides a calibration for the absolute sweep rate.

The x-ray drive temperature for this example starts at about 140 eV, and rises to $>200\text{ eV}$. Simulations of the foil trajectory were done using a measured x-ray drive with the Lasnex computer code [6]. Fully corrected measurements are plotted in Figure 11 with the simulated foil position.

4.2 Turn-on time of the hohlraum x-ray drive

The Dante diagnostic is used to measure the x-ray drive temperature in a hohlraum. It consists of an array of filtered x-ray detectors that are recorded with fast transient digitizers. The time-response is about

150 ps, and it has a timing uncertainty of about 100 ps, which limits our ability to measure the fast rise of soft x-ray emission inside the hohlraum.

We used the soft x-ray imager (SXI) to measure the absolute turn-on time of 500 eV soft x-ray emission from an un-illuminated region of the inner hohlraum wall. The SXI consists of a grating spectrometer in combination with a pinhole imager mounted on the front of the SSC. It was aligned to view the inner wall of the hohlraum through a diagnostic hole. In order to precisely characterize the turn-on time of soft x-ray emission inside the hohlraum, we used one Nova beam with a 100 ps pulse as a fiducial beam by pointing it to the outside of the hohlraum within the field of view of the SXI. We viewed the 500 eV emission from the outer wall due to the 100 ps beam simultaneously with the 500 eV emission from the inner wall viewed through the diagnostic hole.

Assuming the soft x-ray emission is prompt from the 100 ps beam, this gives us an accurate measurement of the turn-on time of the soft x-ray wall emission inside the hohlraum. The turn-on of the x-ray emission is shown in Figure 12. Including the effect of the image curvature on the streak camera image, we observed that 500 eV emission starts only 10 ps after the start of the laser pulse.

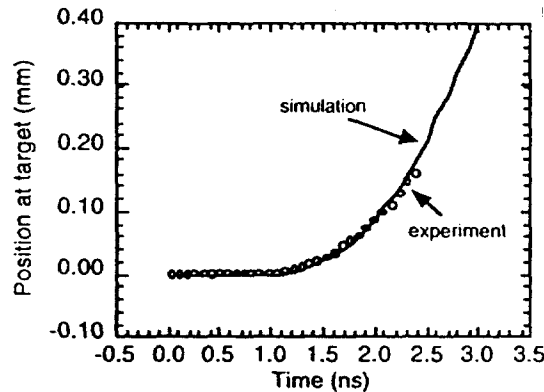


Figure 11: Comparison of the measured foil trajectory with simulation.

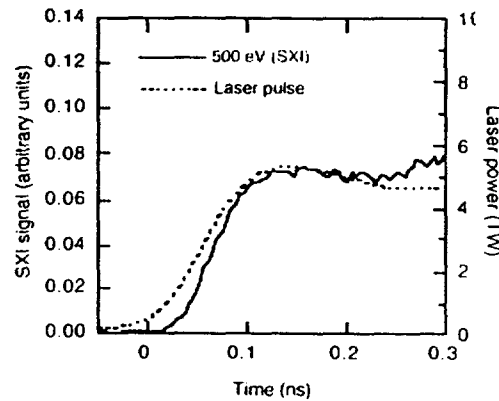


Figure 12: Turn-on of 500 eV emission measured with the SXI and compared with the laser pulse.

5. SUMMARY

We use Nova target shots to characterize the dynamics of the sweep for the SSCs. By using a self-beating laser pulse we generate an x-ray comb. By placing an array of thin slits in front of the photocathode, we record time-space calibration information about the full phosphor screen with a single shot. This information may then be analyzed and applied for quantitative analysis of data recorded with the streak cameras.

6. ACKNOWLEDGMENTS

This work was performed under the auspices of the U.S. D.O.E. by the Lawrence Livermore National Laboratory under Contract No. W-7405-ENG-48.

7. REFERENCES

- [1] B. A. Hammel, P. Bell, C. J. Keane, R. W. Lee, and C. L. S. Lewis, *Rev. Sci. Instrum.* **61**, 2774 (1990).
- [2] Kentech Instruments, Ltd., South Moreton, Didcot, Oxfordshire, OX11 9AG, UK, 44 1 235 510 748.
- [3] O. L. Landen, R. A. Lerche, R. G. Hay, B. A. Hammel, D. Kalantar, and M. D. Cable, *Rev. Sci. Instrum.* **66**, 788 (1995).
- [4] P. Jaanamagi, private communication, 1995.
- [5] H. N. Kornblum, R. L. Kauffman, and J. A. Smith, *Rev. Sci. Instrum.* **57**, 2179 (1986).
- [6] G. B. Zimmerman and W. L. Kruer, *Comments Plasma Phys. Controlled Fusion* **2**, 51 (1975).